nature geoscience

SUPPLEMENTARY INFORMATION

DOI: 10.1038/NGEO1245

Significant contribution of insolation to Eemian melting of the Greenland ice sheet

W. J. van de Berg, M. R. van den Broeke,
J. Ettema, E. van Meijgaard
and F. Kaspar

Supplementary Materials

1 Orbital parameters and greenhouse gas concentrations

Table S1 lists the settings of orbital parameters and greenhouse gas concentrations in the various ECHO-G and RACMO2/GR simulations. The concentrations of trace gases CFC-11 and CFC-12 were set to zero. For an easy comparison of seasons, the date of the vernal equinox (the spring point) was kept fixed for both orbital settings.

ECHO-G and RACMO2/GR were run with a 360-day calendar. Traditional definitions of seasons and month are not equivocal under altered orbital conditions and shortened calendar years. In the main text, all months and seasons are considered to be 30 and 90 days long, respectively. For example, June and summer extend from day 151 to 180 and from day 151 to day 240, respectively.

2 ECHO-G model description

The ECHO-G model consists of the ECHAM4 atmosphere model coupled to the HOPE-G ocean model. The atmosphere model has a horizontal resolution of T30, i.e. approximately 3.75°, and 19 levels in the vertical. The individual simulations comprise several thousand years. The forcing data for the regional climate model have been taken from simulation year 300 onwards. Analysis of ECHO-G model data showed that the climate simulated by ECHO-G has significant decadal variability. Periods with a representative 30 year-mean climate within the whole ECHO-G run were chosen for the RCM simulations. Kaspar and others (2005, 2007) and Kaspar and Cubasch (2007) describe these Eemian ECHO-G simulations in detail.

Table S1: *Prescribed orbital parameters and concentrations of long-lived greenhouse gases.*

	Orbital parameters			Greenhouse gas concentrations		
	Eccentricity	Obliquity [°]	Angle of perihelion [°]	CO_2 [ppmv]	CH_4 [ppmv]	N_2O [ppbv]
125 kyr BP	0.0400	23.79	127.3	270	630	160
PI	0.0167	23.44	282.7	270	600	270

3 RACMO2/GR model adjustments

The following adjustments to the original model formulation have been included to better represent the conditions in the Arctic region (RACMO2/GR).

RACMO2/GR calculates the surface turbulent heat fluxes from Monin-Obukhov similarity theory. An effective surface roughness length is used to account for the effect of small-scale surface elements on turbulent transport. Originally, the roughness lengths for momentum, heat, and humidity (z_{0m}, z_{0h}, z_{0q}) included the effect of enclosing vegetation, urbanisation and orography. This approach gave too large values over the Antarctic ice sheet (Reijmer and others, 2004). For the GrIS, z_{0m} was limited to 100 mm for the tundra without snow and to 1 mm for snow-covered tundra. The value of z_{0m} at the snow covered ice sheet is also set to 1 mm, while z_{0m} is set to 5 mm if bare glacier ice is at the surface (Smeets and Van den Broeke, 2008a). The roughness lengths for heat and moisture over snow surfaces follow Andreas (1987), slightly modified for bare ice areas on the ice sheet (Smeets and Van den Broeke, 2008b). Antarctic experiments have shown that the original model configuration overestimates liquid precipitation at the expense of solid precipitation (Van de Berg and others, 2006). By imposing clouds with temperatures below 267 K to form snow only, the solid precipitation flux increases while leaving the total precipitation sum unchanged. This correction only affects the lower areas of the ice sheet.

The original ECMWF surface scheme does not make a distinction between snow on an ice sheet and seasonal snow cover on the tundra. We introduced an additional surface ice sheet tile in the land surface scheme that treats meltwater percolation, retention and refreezing in the upper 30 m of the snowpack (Figure S1) using a 1D snow/ice model with dynamic layers. The ice temperature at the lowest level is kept constant, assuming no heat flux through the lower boundary. The optimal thickness of a snow/ice layer increases linearly from 6.5 cm at the surface to 4 m at 30 m depth. The layer thickness is continuously changing due to snow accumulation, sublimation, melting, refreezing and firn densification. The vertical grid is adjusted by layer splitting when the layer thickness becomes more than 1.3 times its optimal thickness, or layer fusion when a layer is less than half of its optimal thickness. The lowest layer is duplicated if the snowpack thickness becomes less than 30 m. The number of layers ranges from 35 to 45. Snow density changes due to refreezing of capillary water (rain and meltwater) and the settling and packing of dry snow.

The surface 'skin' temperature, obtained from the surface energy balance (SEB) serves as boundary condition for the englacial module. This module calculates the vertical conduction of heat in a heterogeneous medium. Meltwater and rain are allowed to percolate into the firn until they refreeze or run off. The maximum retention capacity due to capillary forces is set to a low value of 2% of available pore space, to obtain a realistic densification rate by refreezing of capillary water (Greuell and Konzelman, 1994). If the snow/firn pack is saturated with water, the remaining water runs off without delay. Fresh snow has an albedo of 0.825 and a density of 300 kg m^{-3}, glacier ice has an albedo of 0.5 and a density of 900 kg m^{-3}. It between, the snow albedo is coupled to snow density following Greuell and Konzelman (1994), and is limited to a minimum value of 0.7 (Stroeve and others, 2005).

RACMO2/GR has been extensively validated for the current climate. Ettema and others (2009, 2010) showed that RACMO2/GR accurately simulates the present-day climate of the GrIS: the bias in the annual mean 2 m temperature is only +0.9 °C (r = 0.99) and the present-day SMB correlates very well with observations from snow pits and firn cores (r = 0.95).

4 Simulation set-up testing

The results presented are all performed using single nesting, as described in the methods section. Tests were also performed using double nesting, in which RACMO2/GR was first run at 0.5° ($\approx$ 55 km)

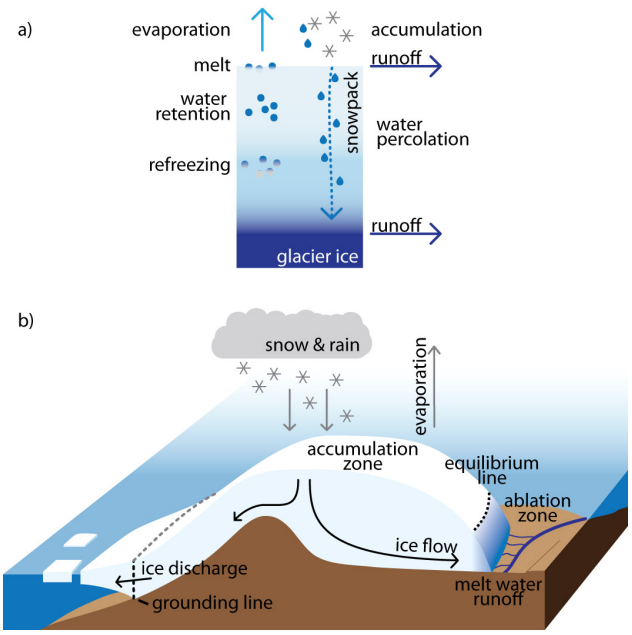

Fig. S1: *Schematic illustration of a) snowpack processes in the melt zone; b) ice sheet mass balance processes.*

resolution in an area of about 6000 by 7000 km centered around Greenland. Results of this experiment were then used to drive the experiment at the final resolution (0.165°, $\approx$ 18 km), with wide relaxation zones positioned well away from the Greenland coast. These tests did not significantly change the results.

5 Assessing the quality of the Preindustrial experiment

To assess whether ECHO-G boundary conditions provide a realistic estimate of GrIS SMB, the Preindustrial (PI) experiment is compared to a present-day (1961-1990) assessment of GrIS SMB (Table 1, Fig. S2). This assessment (Ettema and others, 2009) was made using the same regional model, but at still higher horizontal resolution (11 km) and using lateral forcing fields that include assimilated meteorological observations (ECMWF Re-Analysis data, ERA-40). Compared to the present-day, the PI experiment simulates a 2 K lower annual mean 500 hPa temperature over Greenland, which is not unrealistic (Box and others 2009). This results in reduced melt, refreezing and runoff, but also reduced precipitation (Table 1). Since these effects partly cancel, the SMB is reduced by only 7% compared to the present-day. The SMB change over the ice sheet is rather uniform, and spatial SMB patterns for the PI and present are very similar (Fig. S2).

6 Interpretation of the results in terms of surface energy balance

To interpret the results of the sensitivity experiments it is imperative to make a clear distinction between forcing and response. Two major forcings enhance GrIS summer melt in the Eemian compared to the PI: (1) a greater downward flux of shortwave radiation and (2) a warmer ambient atmosphere, resulting in a greater downward flux of longwave radiation. The acronyms *Eem_Ins* (mimicking forcing 1) and *Eem_Temp* (mimicking forcing 2) thus refer to the forcing at the model boundaries, not to the response

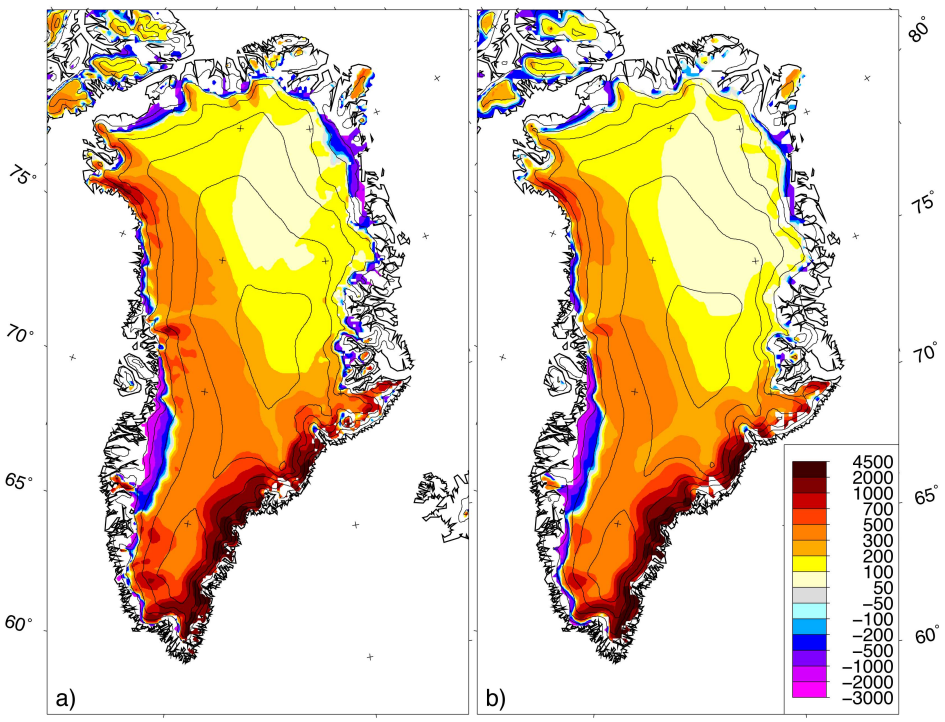

Fig. S2: *Surface mass balance (kg m^{-2} yr^{-1}), for a) 1961–1990 (Ettema and others, 2009) and b) Preindustrial. The SMB color scale is equal for both figures. Ice sheet elevation contours are given at 500 m intervals.*

at the surface of the ice sheet. The concentration of greenhouse gases was also different in the Eemian compared to the PI (Table S1); this small forcing is included in the *Eem_Temp* experiment.

In both the *Eem_Ins* and *Eem_Temp* experiments, the energy flux towards the surface is enhanced relative to the PI. If the surface temperature of the ice sheet is below the melting point, this forcing will heat the surface. The lower atmosphere, which is coupled to the surface through heat exchange by turbulent mixing and longwave radiation transport, will subsequently also heat up (atmospheric adjustment). If the surface of the ice sheet reaches the melting point, it cannot increase its temperature further, limiting further atmospheric adjustment; rather, the additional energy is invested in melting. When snow is at the surface, this melting will lower the albedo, a process also referred to as the snowmelt-albedo feedback. All these adjustments at the surface and in the atmosphere are part of the response that we are interested in, and should not be interpreted as additional forcings.

For this study, our main interest lies in the melt response ΔM, which is determined by changes in the surface energy balance at the snow/ice surface:

$$\Delta M = \Delta SW_{net} + \Delta LW_{net} + \Delta SHF + \Delta LHF + \Delta G_s \quad (\text{in Wm}^{-2})$$

where Δ represents the change relative to the PI, M is melt energy, SW_{net} is absorbed shortwave radiation, LW_{net} is net longwave radiation, SHF and LHF are the turbulent fluxes of sensible and latent heat, respectively, and G_s is the subsurface conductive heat flux. Figure S3 shows the seasonal variation of ΔM, ΔSW_{net}, ΔLW_{net} and the summed contribution of the residual components ($\Delta SHF + \Delta LHF + \Delta G_s$), area-averaged for the (PI) runoff zone, for (a) *Eem_Ins*, (b) *Eem_Temp*, (c) *Eem_Ins* + *Eem_Temp* and (d) the full Eemian experiment. Fig. S4 shows the seasonal variation of albedo for the four experiments, also area-averaged for the (PI) runoff zone.

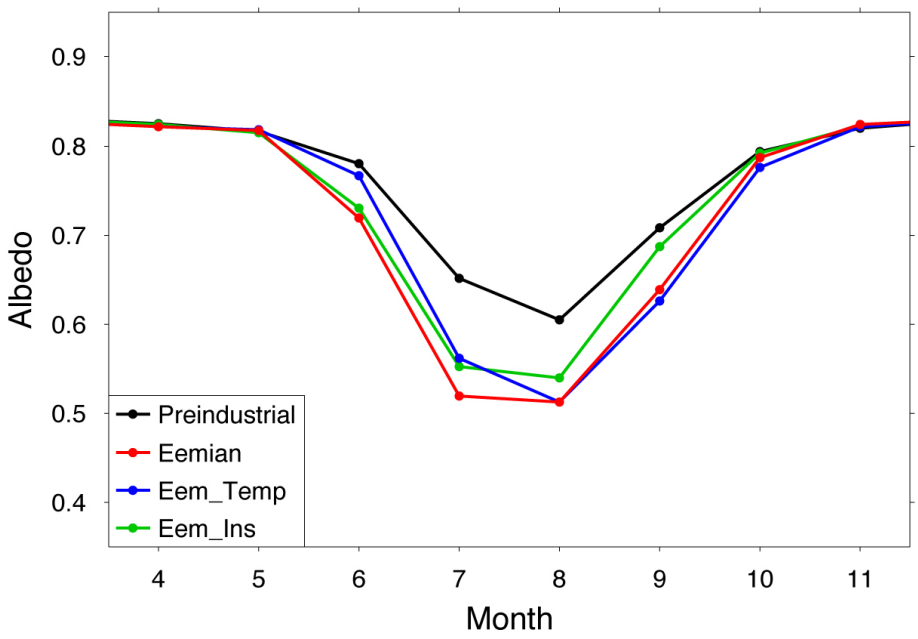

Fig. S3: *Seasonal evolution of surface albedo in the Preindustrial runoff zone. The albedo is calculated as the ratio of the time-averaged area-mean of incoming and reflected shortwave fluxes.*

In the *Eem_Ins* experiment (Fig. S3, Fig. S4a), melting is enhanced primarily in June and July, the months in which insolation increased most significantly compared to the PI (Fig. 1). The increase in melting energy (ΔM) is fully accounted for by ΔSW_{net}, in spite of local atmospheric adjustment. This complies with the assumption that the lower atmospheric adjustment is part of the response, not of the forcing. Note the significant drop in albedo in *Eem_Ins* compared to the PI (Fig. S3), which indicates that the snowmelt-albedo feedback has further enhanced ΔSW_{net} and therewith ΔM.

The forcing in *Eem_Temp* is from enhanced downward longwave radiation, which is visible as a significant contribution of ΔLW_{net} to ΔM in Fig. S4b. However, ΔSW_{net} again dominates the response. This time ΔSW_{net} is fully accounted for by the snowmelt-albedo feedback, because incoming SW remains unchanged in *Eem_Temp* compared to the PI. Apparently the melt-albedo feedback is important under all forcing scenario's. In contrast to *Eem_Ins*, a significant increase in melting also occurs in August, because the forcing in *Eem_Temp* principally derives from excess heating of the surrounding continents and oceans, which is a relatively slow process and lags the insolation anomaly.

Fig. S4c shows the sum of the changes in *Eem_Ins* and *Eem_Temp*. The result is very similar to the changes in the full Eemian experiment (Fig. S4d). The summed changes in SW_{net} slightly exceed those in the full Eemian experiment, because the snowmelt-albedo feedback is counted twice, while in the full Eemian experiment the model albedo cannot drop below 0.5 once ice is at the surface (see Fig. S3 and the negative values in the ablation zone in Fig. 3c).

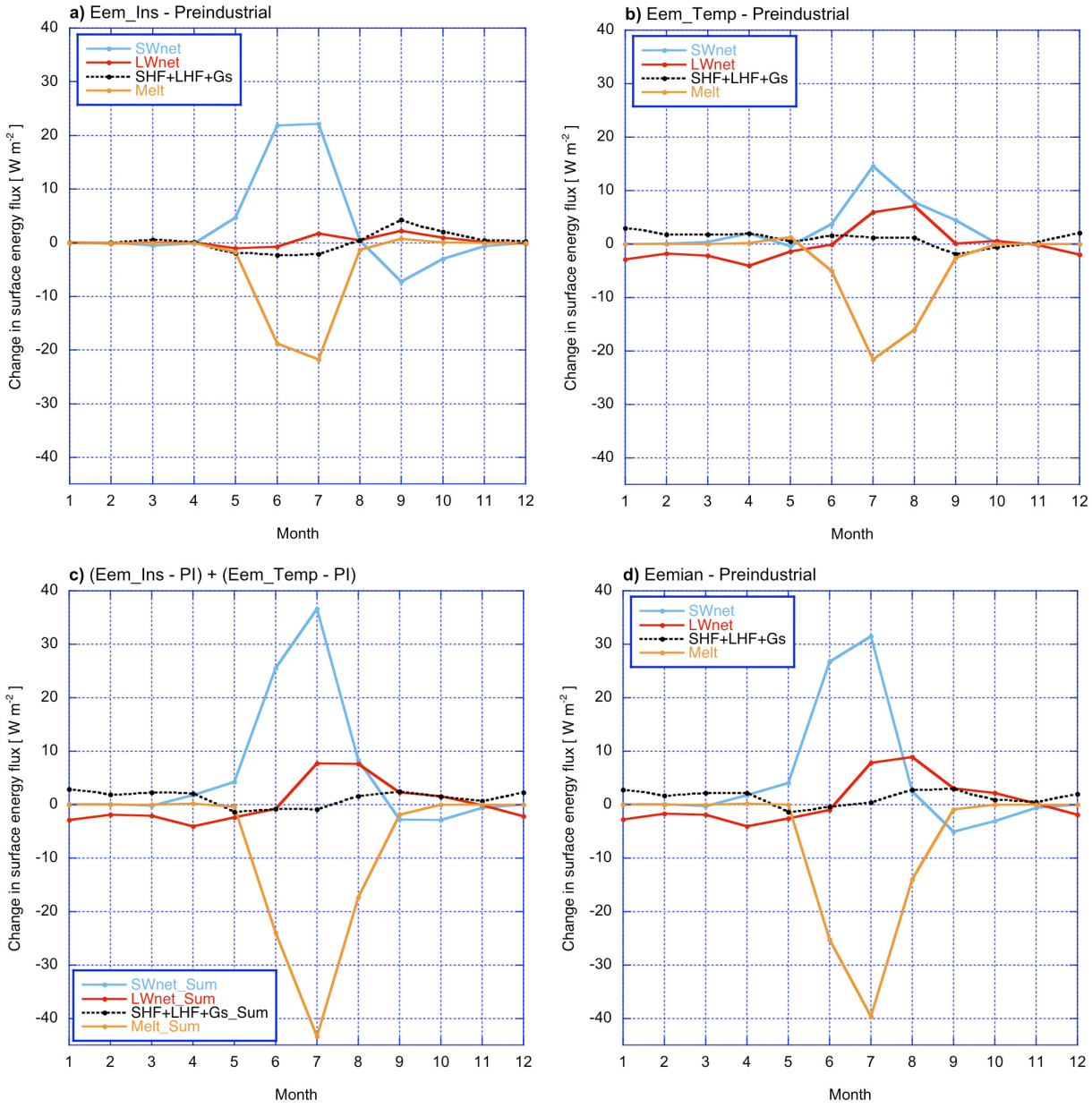

Fig. S4: *Seasonal evolution of changes in surface energy balance components, relative to the Preindustrial vales and averaged over the Preindustrial runoff zone, for (a)* Eem_Ins*, (b)* Eem_Temp*, (c) the sum of these two and (d) the full Eemian experiment.*

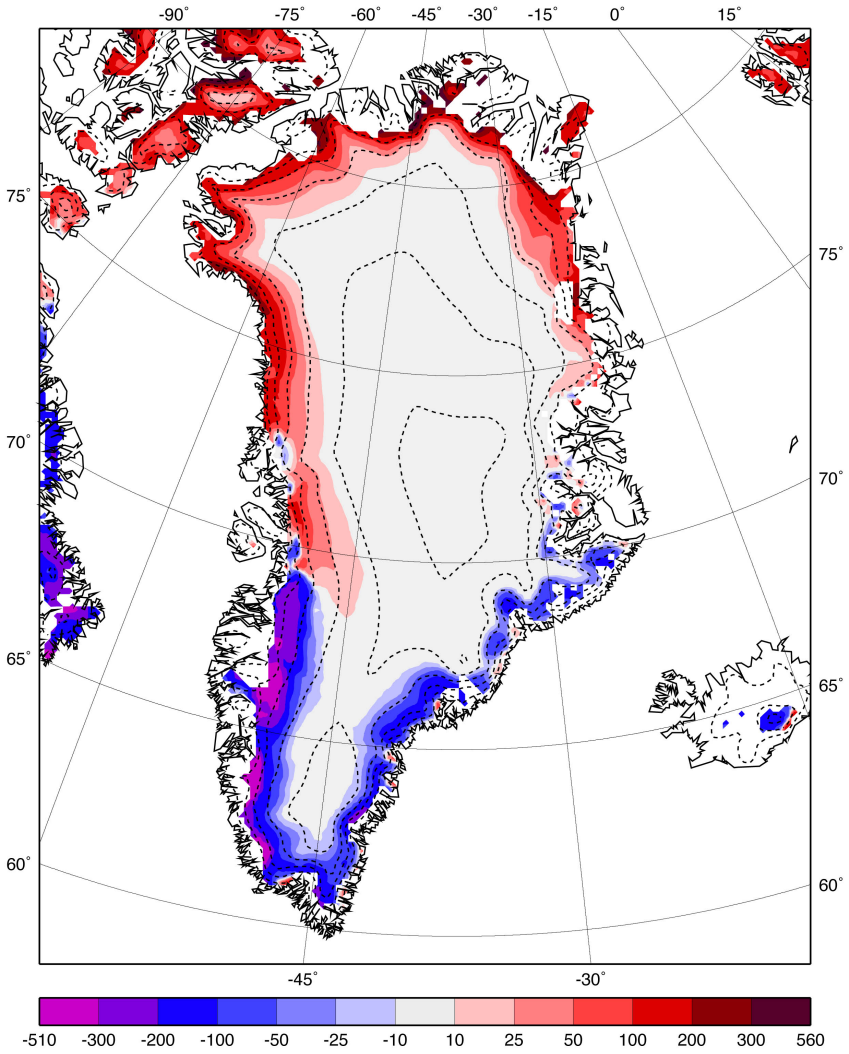

Fig. S5: *Difference in annual melt rate (kg m^{-2} yr^{-1}) between the Preindustrial run of the full model and the calculation based on optimized PDD factors.*

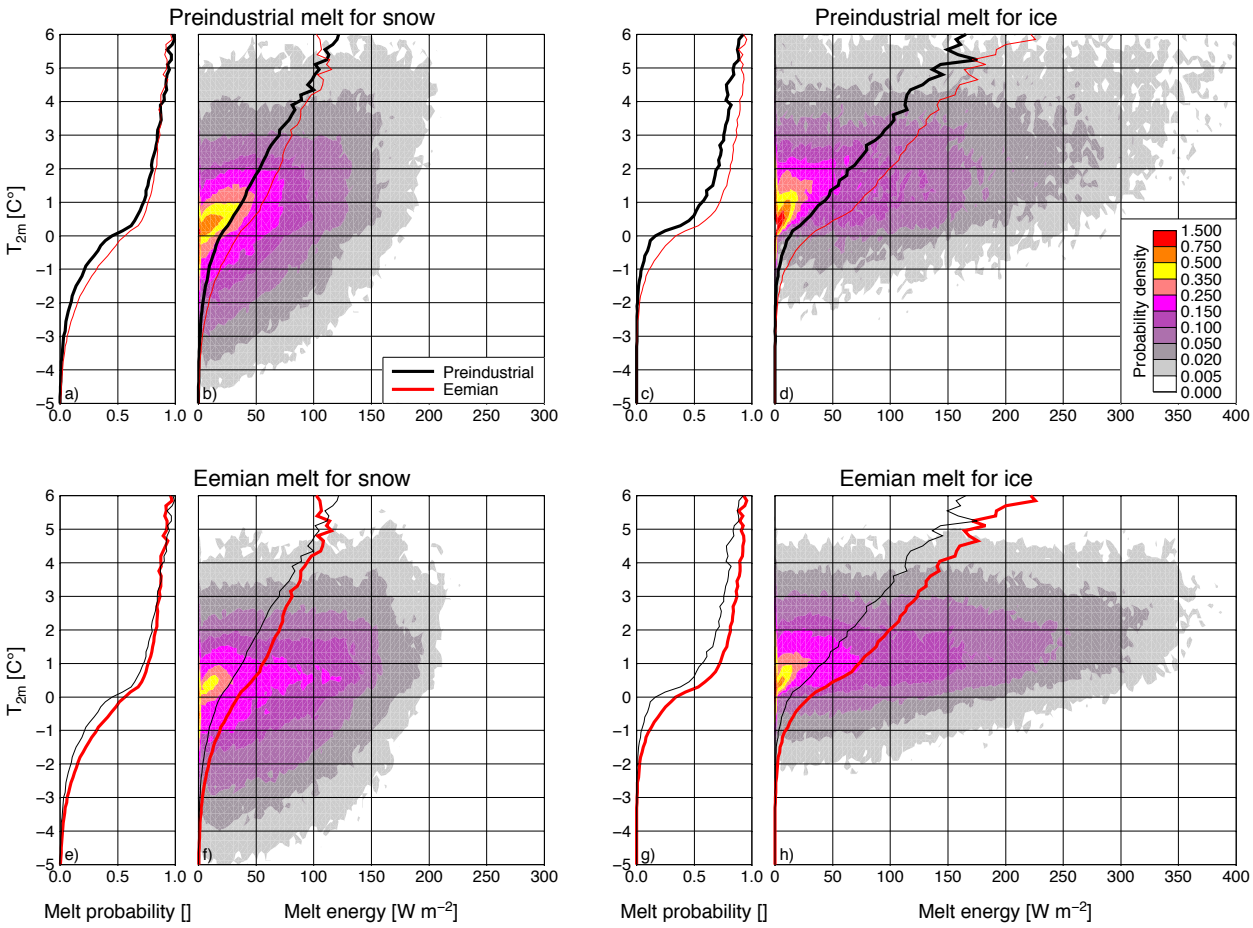

Fig. S6: *Probability of melt as function of T_{2m} (a,c,e,g) and probability density functions of melt energy events (b,d,f,h) for preindustrial (a-d) and Eemian (e-h) insolation and over snow (a,b,e,f) and ice (c,d,g,h). Melt energy probabilities in (b,d,f,h) are scaled and sum up to 100. In (b,d,f,h), mean melt energy for snow/ice as function of T_{2m} are shown with black and red lines for preindustrial and Eemian insolation, respectively. One year of three-hourly instantaneous local surface energy balance values and T_{2m} are used for this Figure.*

Supplementary references

Andreas, E. L.. 1987: A theory for the scalar roughness and the scalar transfer coefficients over snow and sea ice. *Boundary-Layer Meteorology* **38**, 159–184.

Box, J. E., L. Yang, D. H. Browmich and L-S. Bai, 2009: Greenland ice sheet surface air temperature variability: 1840-2007. *J. Clim.* **22**, 4029–4049.

Ettema, J., M. R. van den Broeke, E. van Meijgaard, W. J. van de Berg, J. E. Box and K. Steffen, 2010: Climate of the Greenland ice sheet using a high-resolution climate model, Part 1: Evaluation. *Cryosphere Discuss.* **4**, 561-602.

Greuell, W. G. and T. Konzelmann, 1994: Numerical modelling of the energy balance and the englacial temperature of the Greenland Ice Sheet. Calculations for the ETH-Camp location (West Greenland, 1155 m a.s.l.). *Glob. Planet. Change* **9**, 91-114

Kaspar, F., T. Spangehl and U. Cubasch, 2007: Northern hemispheric winter storm tracks of the Eemian interglacial and the last glacial inception. *Clim. Past* **3**, 181-192.

Reijmer, C. H., E. van Meijgaard and M. R. van den Broeke, 2004: Numerical studies with a regional atmospheric climate model based on changes in the roughness length for momentum and heat over Antarctica. *Bound. Layer Meteorol.* **111**, 313-337.

Smeets, C. J. P. P. and M. R. van den Broeke, 2008a: Temporal and spatial variation of momentum roughness length in the ablation zone of the Greenland ice sheet. *Boundary-Layer Meteorol.* **128**, 315-338.

Smeets, C. J. P. P. and M. R. van den Broeke, 2008b: The parameterisation of scalar transfer over rough ice surfaces. *Bound. Layer Meteorol.* **128**, 339-355.

Stroeve, J., J. E. Box, F. G., S. Liang, A. Nolin, C. Schaaf, 2005: Accuracy assessment of the MODIS 16-day albedo product for snow: comparisons with Greenland in situ measurements. *Rem. Sens. Env.* **94**, 46-60.

Van de Berg, W. J., M. R. van den Broeke and E. van Meijgaard, 2006: Reassessment of the Antarctic surface mass balance using calibrated output of a regional atmospheric climate model. *J. Geophys. Res.* **111**, D11104, doi:10.1029/2005JD006495.